

Radiation Transport in Relativistic Magnetized Fluids. Applications to Relativistic Outflows.

J. M. Rueda-Becerril*, P. Mimica, M. A. Aloy and C. Aloy

Department of Astronomy and Astrophysics, University of Valencia

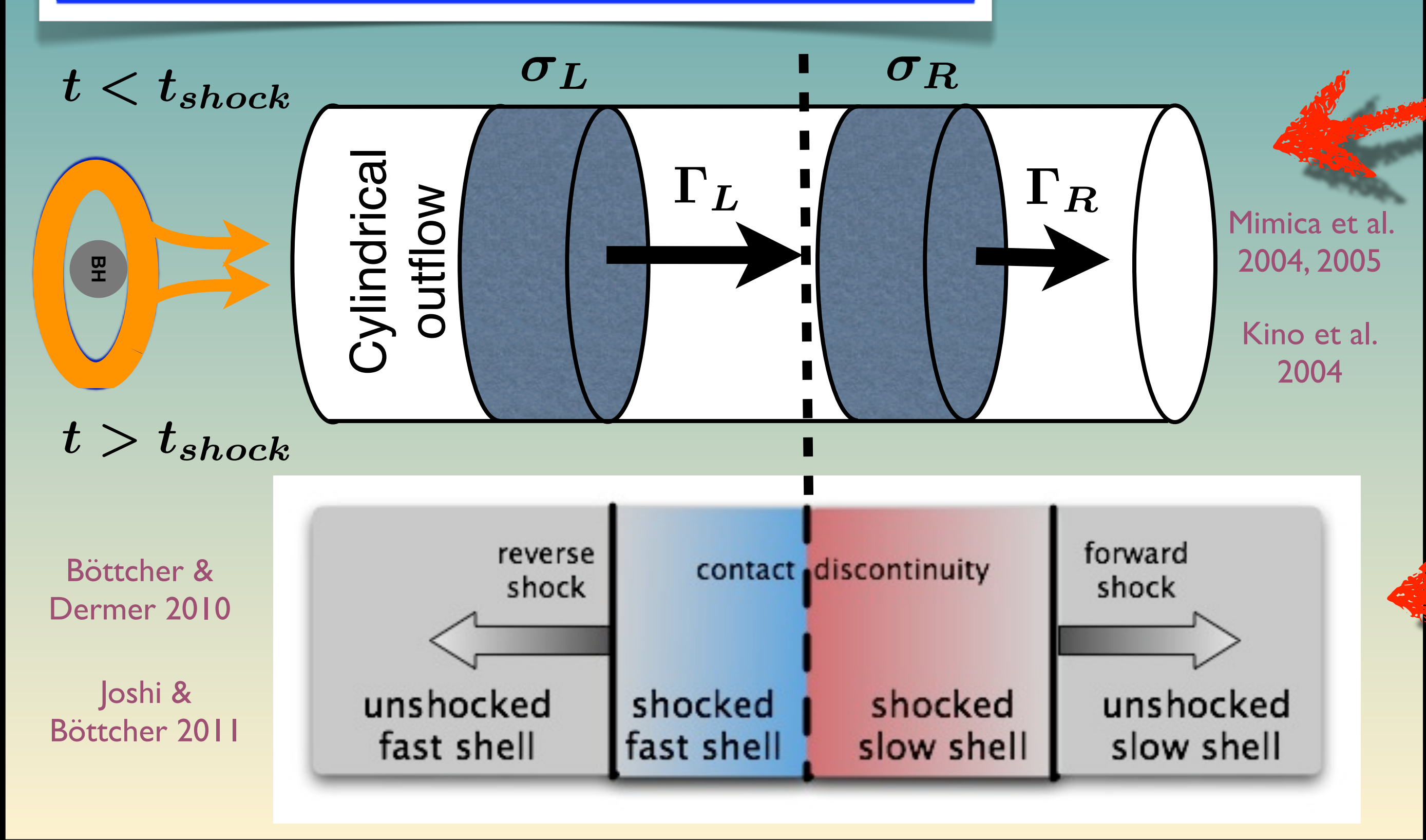
*jesus.rueda@uv.es

1. Introduction

The **internal-shocks** scenario [§2] has been used to explain the variability of blazars' outflow emission (Spada et al. 2001). Recent simulations [§3] have shown that the magnetic field alters the dynamics of these shocks producing a whole zoo of spectral energy density patterns [§4-6]. However, the role played by magnetization in such high-energy emission is still not entirely understood.

With the aid of the 2nd LAT AGN catalog (2LAC), a comparison with observations in the γ -ray band was performed [§7], in order to identify the effects of the magnetic field on the observed spectra.

2.a Magnetized shell collisions



2.b Key definitions

$$\Gamma_L := (1 + \Delta g) \Gamma_R$$

Relative Lorentz factor

$$\sigma := \frac{B^2}{4\pi\rho\Gamma^2 c^2}$$

Magnetization

3. Numerical setup

Riemann problem

Romero et al. 2005

Radiative transfer

Mimica & Aloy 2012

Non-thermal particles transport and evolution (Synchrotron, Inverse Compton)

Mimica et al. 2009

4. Weakly magnetized

$$\sigma_L = \sigma_R = 10^{-6}, \Gamma_R = 10, \theta = 5^\circ$$

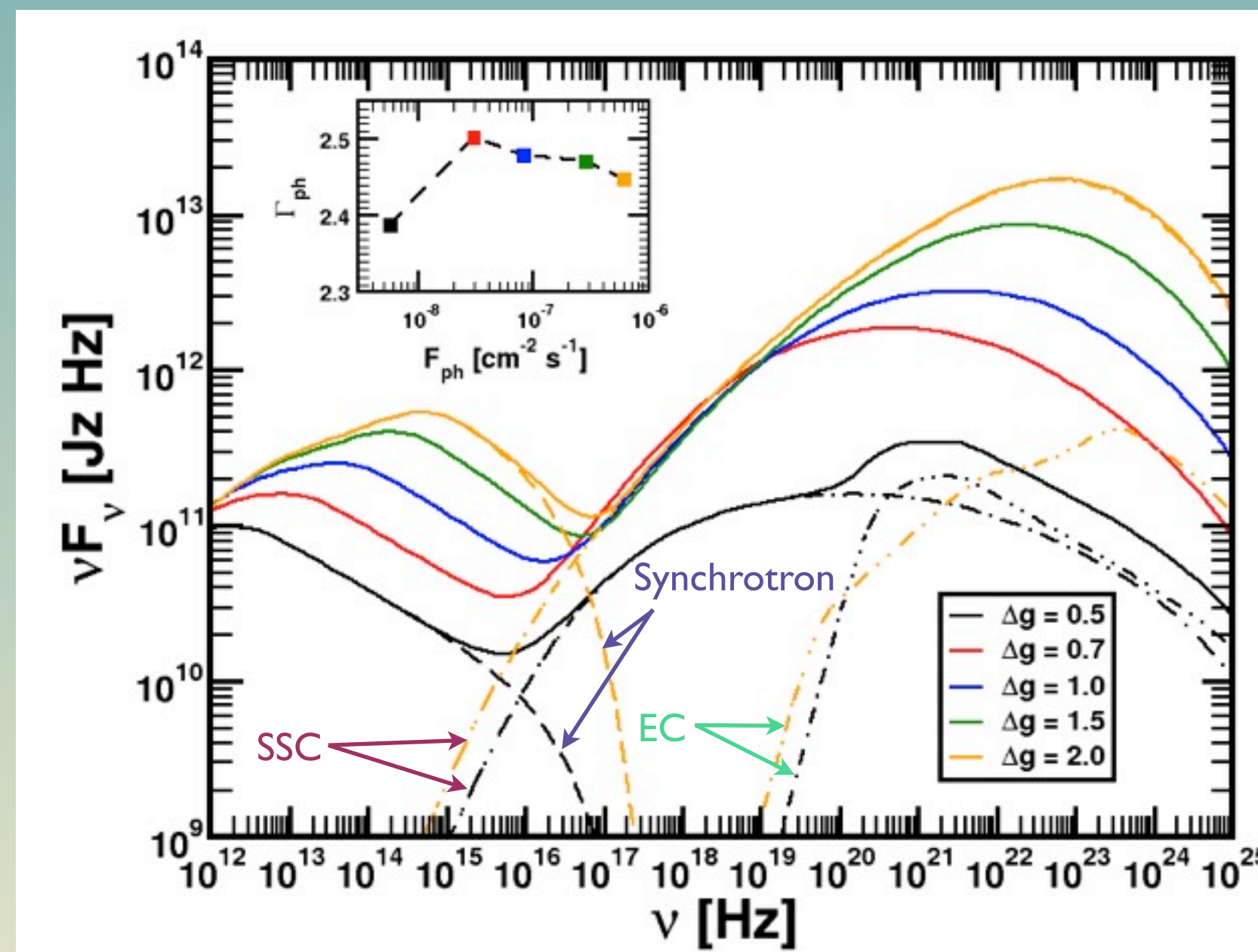


Figure 1. Average spectra. The spectral energy density (SED) of each model has been averaged over the time interval 0–10⁶ s. In addition, for the models $\Delta g = 0.5, 2.0$ we show the **synchrotron**, **synchrotron self-Compton (SSC)** and **external inverse Compton (EIC)** contributions (dashed, dot-dashed and dot-dot-dashed lines, respectively). The inset shows the photon spectral index Γ_{ph} as a function of the photon flux F_{ph} in the γ -ray band. There we can see an almost flat behavior of Γ_{ph} for $\Delta g \geq 0.7$. We use the same band and spectral slope definition as in Abdo et al. 2009.

6. Strongly magnetized

$$\sigma_L = 1, \sigma_R = 0.1, \Delta g = 1.0, \theta = 5^\circ$$

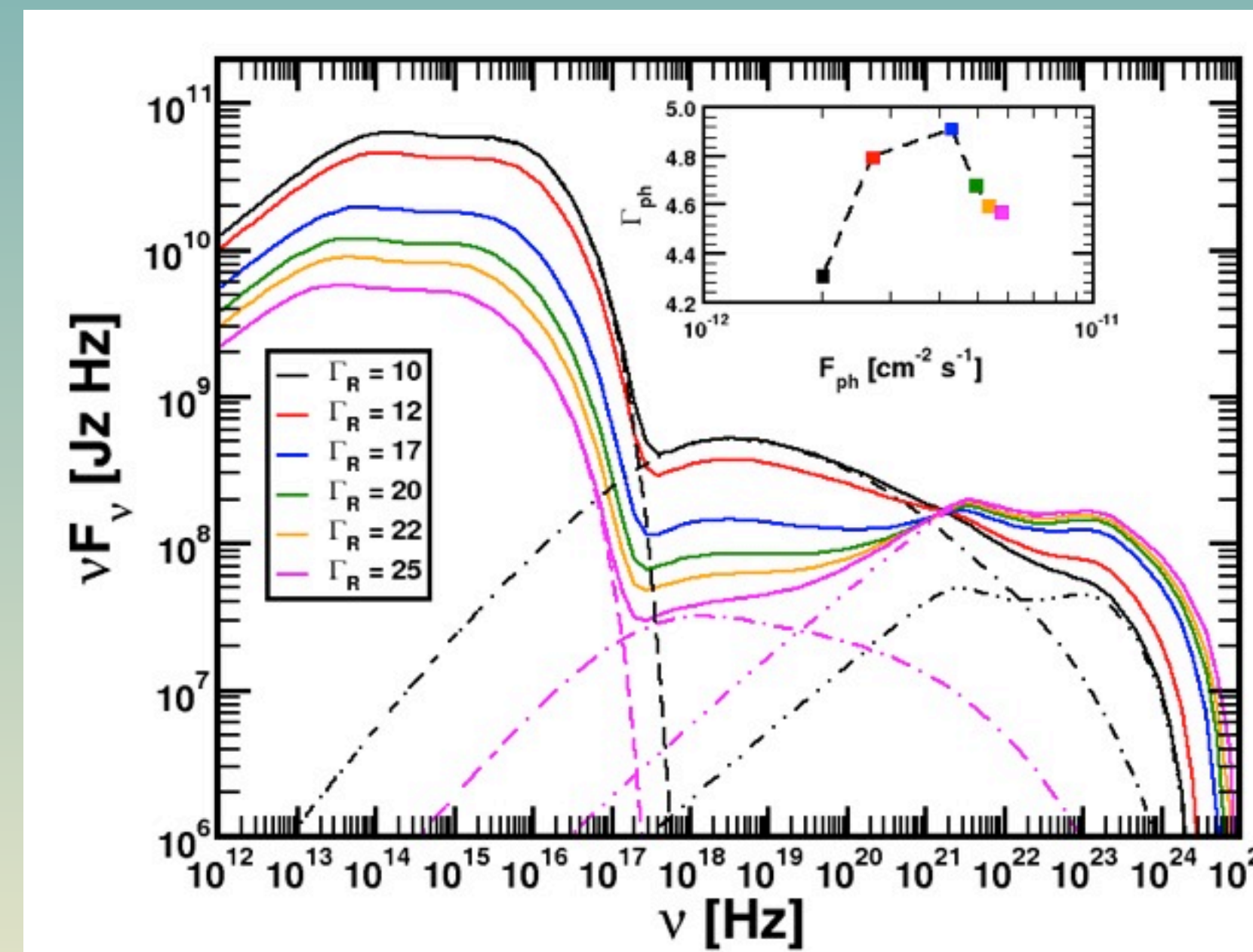


Figure 3. Same as Fig. 2 but for strongly magnetized shells. For the cases with $\Gamma_R = 10, 25$, dashed, dot-dashed and dot-dot-dashed lines show, once more, the **synchrotron**, **SSC** and **EIC** contributions. We can appreciate how the EIC component rises to the point in which it begins to be comparable, in one order of magnitude, to the synchrotron component as Γ_R increases. Again, in the inset we show the photon spectral index Γ_{ph} as a function of the photon flux F_{ph} in the γ -ray band. From there we can observe that an increase in the flux of photons comes with for higher Γ_R along with the decay of the photon index.

8. Doppler factor

$$\sigma_L = \sigma_R = 10^{-2}, \Gamma_R = 10, \Delta g = 1.0$$

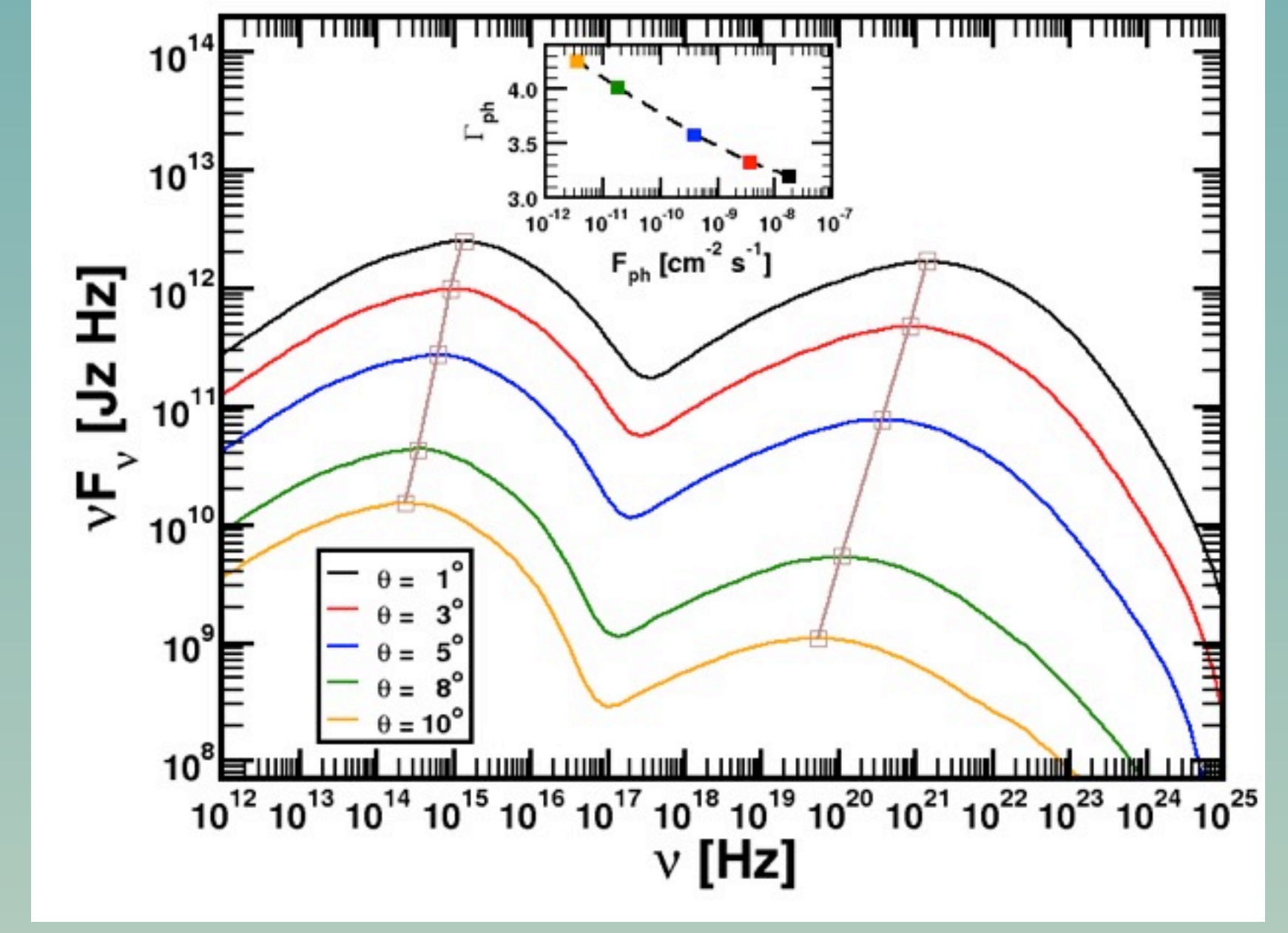


Figure 5. Same as Fig. 2 but for different values of θ . Increasing θ lowers the total emitted flux all over the spectral range. For easier visualization the synchrotron and IC spectral maxima of different models. The decay of the SED's maxima seems to be linear.

$$D := \frac{1}{\Gamma(1 - \beta \cos \theta)}$$

Doppler factor

5. Moderately magnetized

$$\sigma_L = \sigma_R = 10^{-2}, \Delta g = 1.0, \theta = 5^\circ$$

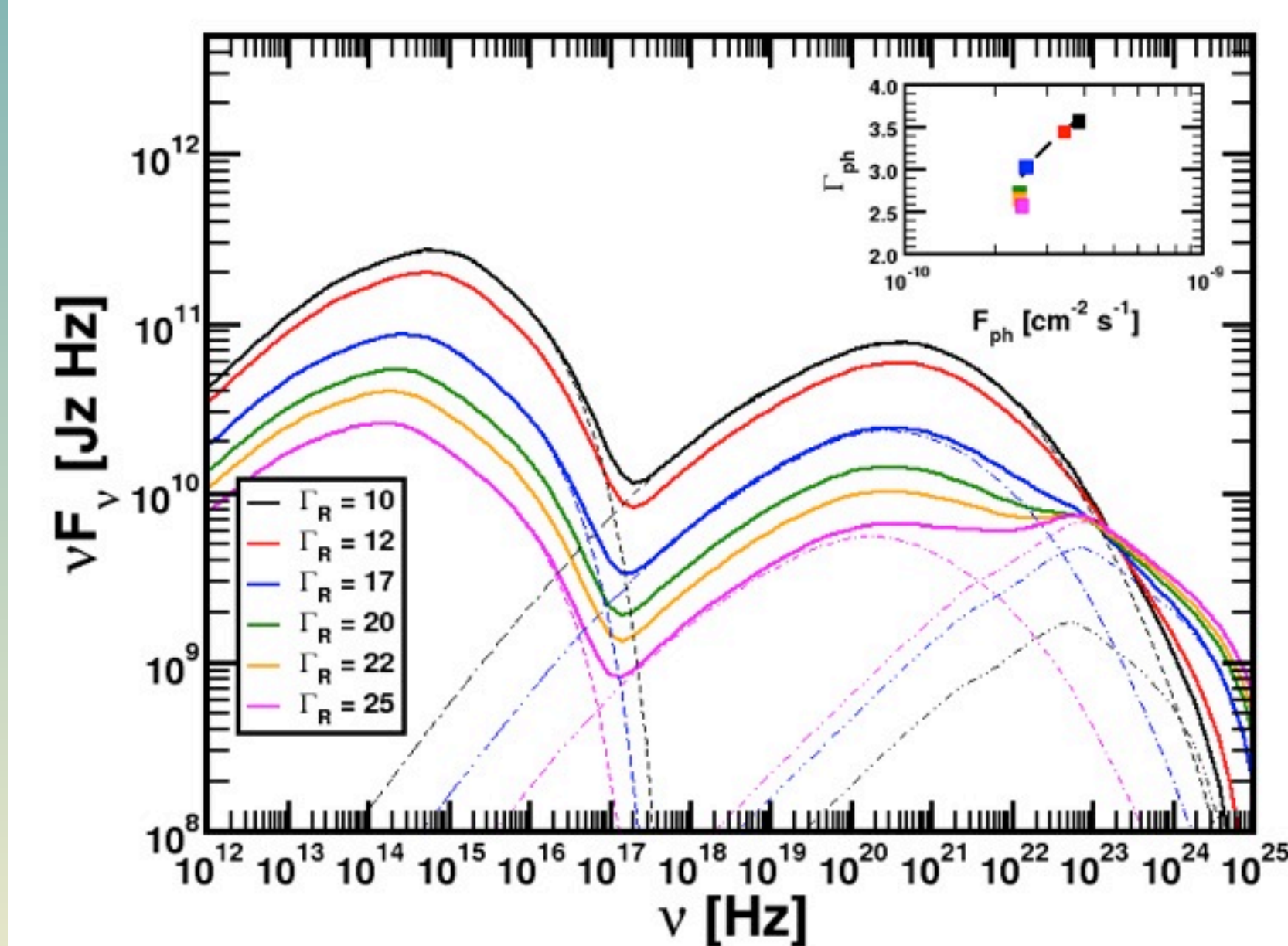


Figure 2. Same class of spectra as Fig. 1 but for a different set of models. For models with $\Gamma_R = 10, 25$, dashed, dot-dashed and dot-dot-dashed lines show, like Fig. 1, the **synchrotron**, **SSC** and **EIC** contributions. Again, in the inset we show the photon spectral index Γ_{ph} as a function of the photon flux F_{ph} in the γ -ray band.

7. Comparing with 2LAC

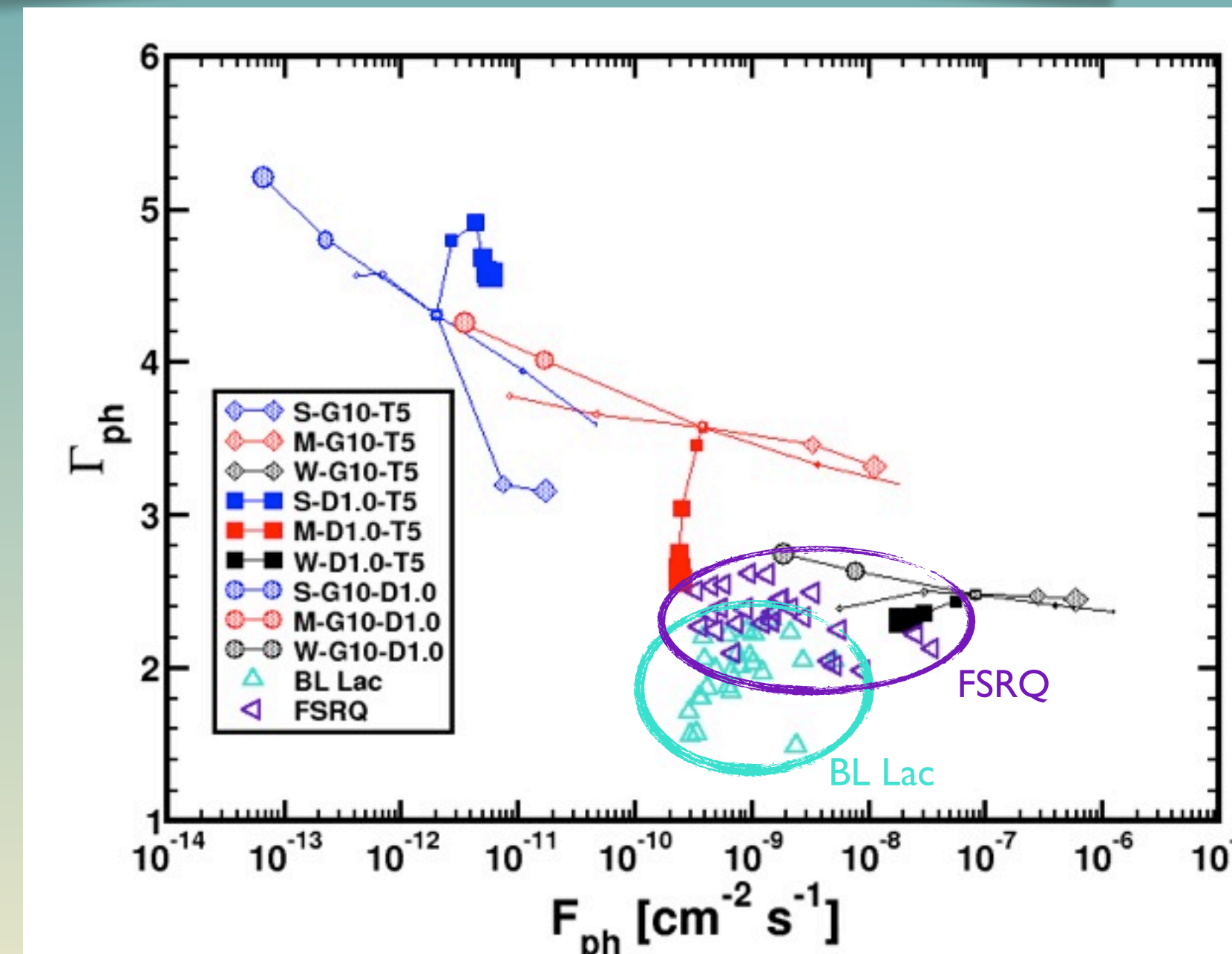


Figure 4. In this figure we present a comparison between our numerical models and those sources (FSRQs and BL Lacs) whose redshift is $z \sim 0.5$ in 2LAC (Ackermann et al. 2011). The horizontal axis (F_{ph}) corresponds to the flux of photons above 100 MeV. The vertical (Γ_{ph}) axis corresponds to the spectral slope of F_{ph} . From the simulations we can identify magnetization regions, being the **weakly magnetized** the ones that overlap with **FSRQs** mostly.

9. Conclusions

When we vary Δg we get a more energetic maximum in the Inverse Compton component, which at the same time is dominated by SSC. When we vary Γ_R we find the opposite: the EIC begins to dominate over SSC, as well as being comparable to the synchrotron component. The increment of θ shows, as expected, a significant decrease (several orders of magnitude between $\theta = 1$ and 10) in the total emitted flux. Among all the models studied the weakly magnetized were the ones that are within *Fermi*'s observational range (Ackermann et al 2011). However, the tendencies of certain models with higher magnetization appear be consistent with the observations.

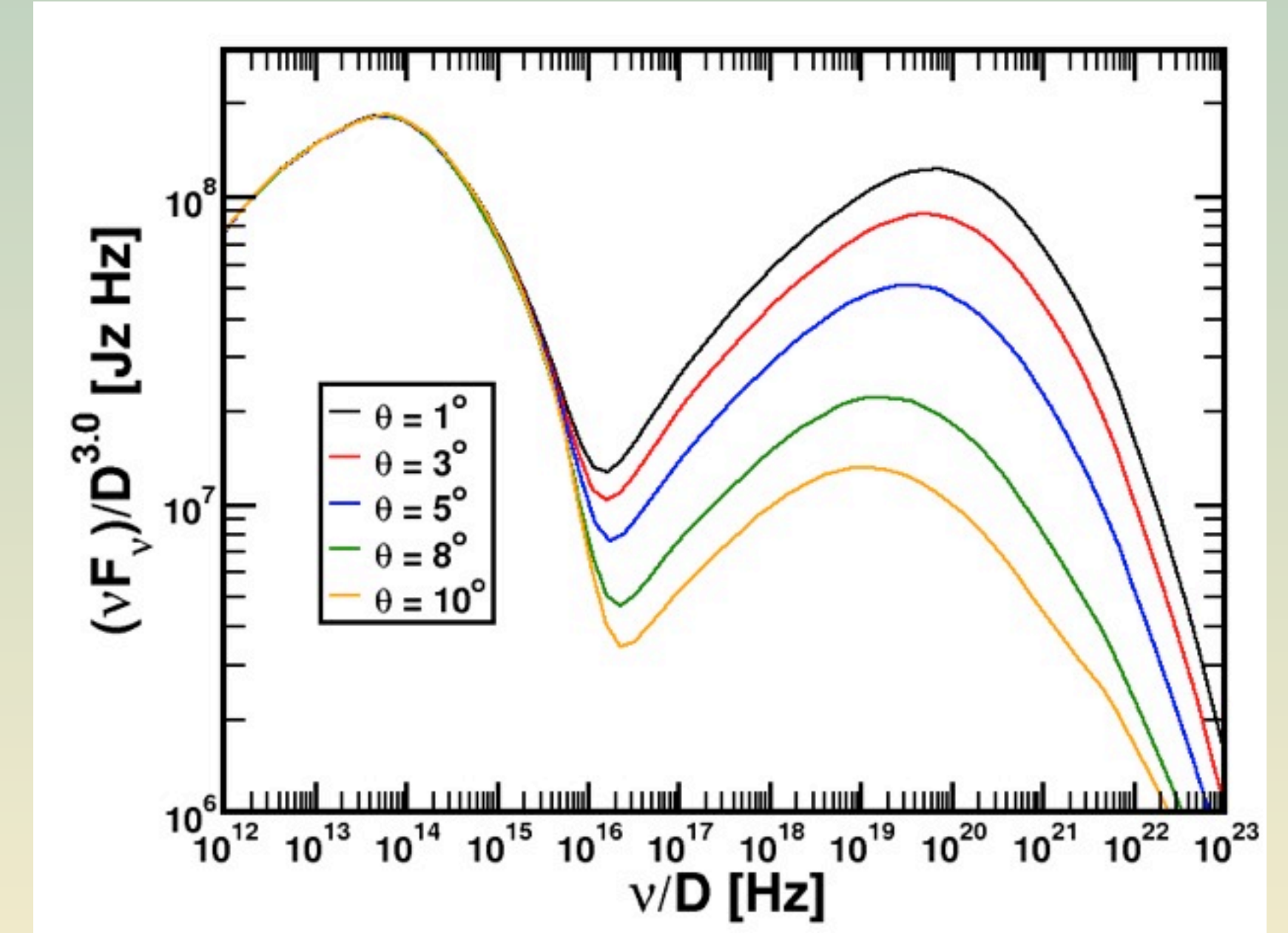


Figure 6. Spectra from Fig. 5 normalized by D^3 . Theoretically, it is known that the beaming pattern of a relativistically moving blob of electrons that Thompson-scatter photons from an external isotropic radiation field changes as $D^{4+\alpha}$ (α being the spectral index of the radiation), while the beaming pattern of radiation emitted isotropically in the blob frame (e.g., by synchrotron and SSC processes), changes as $D^{3+\alpha}$ (Dermer 1995).

References

- Abdo, A. A. et al. 2009, *ApJ*, 700, 597
- Ackermann, M. et al. 2011, *ApJ*, 743, 171
- Böttcher, M. & Dermer, C. D. 2010, *ApJ*, 711, 445
- Dermer, C. D. 1995, *ApJ*, 446, L63
- Joshi, M. & Böttcher, M. 2011, *ApJ*, 727, 21
- Kino, M., Mizuta, A. & Yamada, S. 2004, *ApJ*, 611, 1021
- Mimica, P. & Aloy, M. A. 2012, *MNRAS*, 421, 2635
- Mimica, P. et al. 2009, *ApJ*, 696, 1142
- Mimica, P., Aloy, M. A., Müller, E. & Brinkmann, W. 2005, *A&A*, 441, 103
- Mimica, P., Aloy, M. A., Müller, E. & Brinkmann, W. 2004, *A&A*, 418, 947
- Romero, R., Martí, J. M., Pons, J. A., Ibáñez, J. M. & Miralles, J. A. 2005, *J. Fluid Mech.*, 544, 323
- Spada, M., Ghisellini, G., Lazzati, D. & Celotti, A. 2001, *MNRAS*, 325, 1559